A Nonlinear Variational Method for Improved Quantification of Myocardial Blood Flow Using $H_2{}^{15}O$ PET

Seminar Wissenschaftliches Rechnen, Kleinwalsertal

Martin Benning
martin.benning@wwu.de

Westfälische Wilhelms-Universität, Münster
Institut für Numerische und Angewandte Mathematik

15.02.09

Table of Contents

Motivation

Motivation

- Cardiovascular diseases are the most common cause of death in industrialized countries

Motivation

- Cardiovascular diseases are the most common cause of death in industrialized countries
- Every year up to 12 million people die due to cardiovascular diseases. More than 50 % of these cases of death could have been prevented by early diagnosis

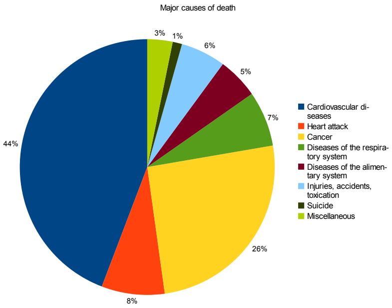

Motivation

- Many cardiovascular diseases originate in atherosclerosis (especially in the cardiovascular vessels)

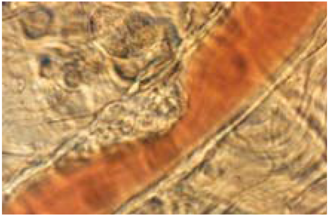

Motivation

- Many cardiovascular diseases originate in atherosclerosis (especially in the cardiovascular vessels)

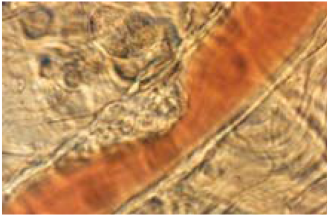

- Typical way of diagnosis: catheterization.

Motivation

- Many cardiovascular diseases originate in atherosclerosis (especially in the cardiovascular vessels)

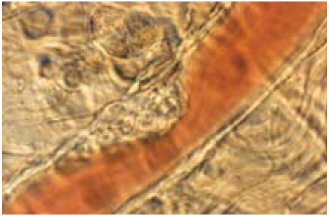

- Typical way of diagnosis: catheterization.
- Disadvantage: invasive and therefore cumbersome for patients; possible risk of thrombosis, embolism, infections or cardiac arrythmia

Motivation

- Many cardiovascular diseases originate in atherosclerosis (especially in the cardiovascular vessels)

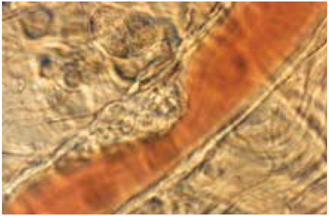

- Typical way of diagnosis: catheterization.
- Disadvantage: invasive and therefore cumbersome for patients; possible risk of thrombosis, embolism, infections or cardiac arrythmia
- Furthermore, detected constrictions must not be the result of plaque, but can have different reasons (potential of false diagnosis)

Motivation

- Alternative: diagnosis via dynamic $H_2{}^{15}O$ Positron Emission Tomography (PET)

Motivation

- Alternative: diagnosis via dynamic $H_2{}^{15}O$ Positron Emission Tomography (PET)

Dynamic $H_2{}^{15}O$ PET

- Dynamic PET allows noninvasive investigation of physiological processes within the body

Dynamic $H_2{}^{15}O$ PET

- Dynamic PET allows noninvasive investigation of physiological processes within the body
- In particular, $H_2{}^{15}O$ as a tracer allows investigation of perfusible tissue

Dynamic $H_2{}^{15}O$ PET

- Dynamic PET allows noninvasive investigation of physiological processes within the body
- In particular, $H_2{}^{15}O$ as a tracer allows investigation of perfusible tissue
- With the use of simple kinetic models, conclusions on perfusion in myocardium and on blood flow in adjacent vessels can be drawn

Dynamic $H_2{}^{15}O$ PET

- Dynamic PET allows noninvasive investigation of physiological processes within the body
- In particular, $H_2{}^{15}O$ as a tracer allows investigation of perfusible tissue
- With the use of simple kinetic models, conclusions on perfusion in myocardium and on blood flow in adjacent vessels can be drawn
- Furthermore $H_2{}^{15}O$ offers a half-life of about 2 min. and therefore adds a small radiation exposure to the patient

Dynamic $H_2{}^{15}O$ PET

- Disadvantage: due to the short half-life of $H_2{}^{15}O$ the quality of reconstructed images is very poor

Dynamic $H_2{}^{15}O$ PET

- Disadvantage: due to the short half-life of $H_2{}^{15}O$ the quality of reconstructed images is very poor

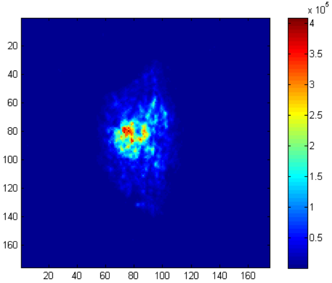

Figure: A 2D $H_2{}^{15}O$ EM reconstruction of a transaxial slice intersecting the cardiovascular region, with added Gaußian smoothing

Dynamic $H_2{}^{15}O$ PET

- A couple of low quality reconstructions provide the basis for postprocessing via a kinetic model to obtain physiological parameters that describe e.g. perfusion

Dynamic $H_2{}^{15}O$ PET

- A couple of low quality reconstructions provide the basis for postprocessing via a kinetic model to obtain physiological parameters that describe e.g. perfusion
- Main drawback is that computation of low quality reconstructions and subsequent postprocessing via a kinetic model is done independently of each other

Dynamic $H_2{}^{15}O$ PET

- A couple of low quality reconstructions provide the basis for postprocessing via a kinetic model to obtain physiological parameters that describe e.g. perfusion
- Main drawback is that computation of low quality reconstructions and subsequent postprocessing via a kinetic model is done independently of each other
- New approach: integrate the process of kinetic modelling into the reconstruction process to compute more accurate parameters (parameters are computed from the PET data and not from low resolution images)

$$\boxed{p(x,t)} \xrightarrow[\text{nonlinear}]{G} \boxed{u(x,t)} \xrightarrow[\text{linear}]{B} \boxed{f(\sigma,\theta,t)}$$

Inversion of

nonlinear operator G

Basic Mathematics for PET

Basic Mathematics for PET

- The basic principle of PET

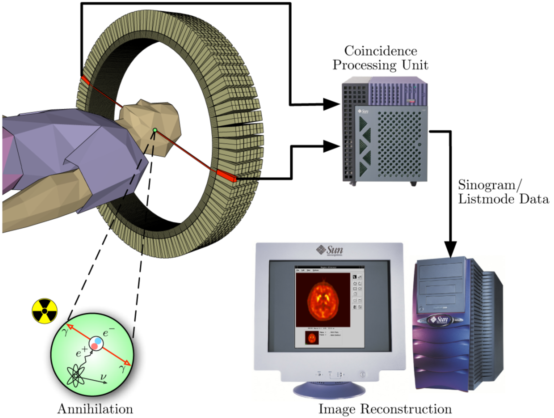

leads to the following inverse problem

The Inverse Problem of PET

The basic inverse problem of PET is to obtain an image $u : \Omega \subset \mathbb{R}^n \to \mathbb{R}$ from the operator equation

$$\wp(Bu) = f\,, \tag{1}$$

where $f : \Sigma \to \mathbb{R}$ is the measured PET data, $\wp$ is an operator guaranteeing Poisson statistics and B is the X-ray transform, defined as

$$(Bu)(\theta, x) = \int_{\mathbb{R}} u(x + t\theta)dt\,, \tag{2}$$

with $\theta \in S^{n-1}$ and $x \in \theta^{\perp}$.

The Inverse Problem of PET

The basic inverse problem of PET is to obtain an image $u : \Omega \subset \mathbb{R}^n \to \mathbb{R}$ from the operator equation

$$\wp(Bu) = f \,, \tag{1}$$

where $f : \Sigma \to \mathbb{R}$ is the measured PET data, $\wp$ is an operator guaranteeing Poisson statistics and B is the X-ray transform, defined as

$$(Bu)(\theta, x) = \int_{\mathbb{R}} u(x + t\theta) dt \,, \tag{2}$$

with $\theta \in S^{n-1}$ and $x \in \theta^{\perp}$.

- In two dimensions, the X-ray transform is equivalent to the Radon transform

EM

- Since positrons are Poisson distributed, the standard approach to solve (1) is to compute the unique and global minimizer

Minimization of Kullback-Leibler functional

$$u \in \arg\min_{u \in \mathcal{U}} KL(f, Bu)\,, \tag{3}$$

with

$$KL(f, Bu) = \int_{\Sigma} f \log\left(\frac{f}{Bu}\right) + Bu - f \, dx\,, \tag{4}$$

in an appropriate function space $\mathcal{U}$ (e.g. $\mathcal{U} = L_2(\Omega)$)

- The minimum of (3) can be computed via

Optimality condition

$$B^* 1 - B^* \left(\frac{f}{Ru} \right) = 0\,. \tag{5}$$

- The minimum of (3) can be computed via

Optimality condition

$$B^*1 - B^*\left(\frac{f}{Ru}\right) = 0\,. \tag{5}$$

- In discrete terms equation (5) can be computed via the standard EM algorithm

Standard EM algorithm

$$u_{k+1} = \frac{u_k}{B^*1}\, B^*\left(\frac{f}{Bu_k}\right)\,, \tag{6}$$

with 1 being the constant 1-function and an initial value $u_0 > 0$.

State-of-the-art MBF Quantification

- To obtain physiological parameters, a sequence of images (frames) has to be computed via (6)

State-of-the-art MBF Quantification

- To obtain physiological parameters, a sequence of images (frames) has to be computed via (6) $\Rightarrow u(x,t)$, for $t \in [0, T]$

State-of-the-art MBF Quantification

- To obtain physiological parameters, a sequence of images (frames) has to be computed via (6) $\Rightarrow u(x,t)$, for $t \in [0,T]$
- Sequence $u(x,t)$ provides the basis for computation of physiological values, as e.g. MBF, via a kinetic model

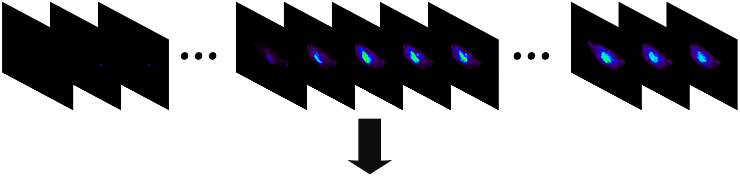

Subsequent parameter computation
via nonlinear fitting

- To apply a kinetic model, segmentation of the cardiovascular region is needed, e.g. via factor images

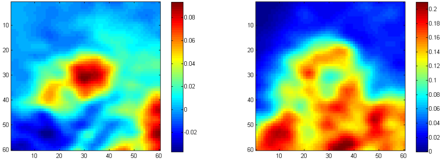

- To apply a kinetic model, segmentation of the cardiovascular region is needed, e.g. via factor images

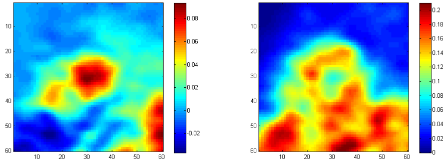

- The cardiovascular region has to be segmented into myocardial tissue, left and right ventricle to extract information on the radioactive distribution in the chambers and to apply a kinetic model to the myocardial tissue region

- To apply a kinetic model, segmentation of the cardiovascular region is needed, e.g. via factor images

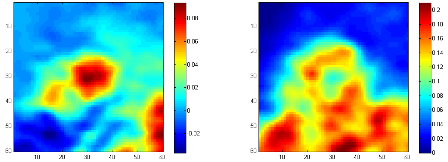

- The cardiovascular region has to be segmented into myocardial tissue, left and right ventricle to extract information on the radioactive distribution in the chambers and to apply a kinetic model to the myocardial tissue region
- In this talk we do not want to adress the problem of segmentation but the challenge of computing parameters with given segmentation from the data instead of the images

- Since we use a rough segmentation in image space we want to introduce some basic notations to differ between the different spatial regions

- Since we use a rough segmentation in image space we want to introduce some basic notations to differ between the different spatial regions

Notation

- Ω denotes the whole image

- Since we use a rough segmentation in image space we want to introduce some basic notations to differ between the different spatial regions

Notation

- Ω denotes the whole image
- $\mathcal{T}$ denotes the region of myocardial tissue

- Since we use a rough segmentation in image space we want to introduce some basic notations to differ between the different spatial regions

Notation

- Ω denotes the whole image
- $\mathcal{T}$ denotes the region of myocardial tissue
- $\mathcal{A}$ represents the left ventricular region

- Since we use a rough segmentation in image space we want to introduce some basic notations to differ between the different spatial regions

Notation

- Ω denotes the whole image
- $\mathcal{T}$ denotes the region of myocardial tissue
- $\mathcal{A}$ represents the left ventricular region
- $\mathcal{V}$ stands for the right ventricular region

- Since we use a rough segmentation in image space we want to introduce some basic notations to differ between the different spatial regions

Notation

- Ω denotes the whole image
- $\mathcal{T}$ denotes the region of myocardial tissue
- $\mathcal{A}$ represents the left ventricular region
- $\mathcal{V}$ stands for the right ventricular region
- $\mathcal{H}$ with $\overline{\mathcal{H}} = \overline{\mathcal{T}} \cup \overline{\mathcal{A}} \cup \overline{\mathcal{V}}$ represents the whole cardiovascular region

- With given segmentation a physiological model has to be applied to the myocardial region

Physiological Models for MBF-Quantification

Physiological Models for MBF-Quantification

- The standard model for MBF quantification is the one-tissue-compartmental model

One-tissue-compartmental model

$$\frac{\partial\, C_{\mathcal{T}}(x,t)}{\partial t} = F(x) \left(C_{\mathcal{A}}(t) - \frac{C_{\mathcal{T}}(x,t)}{\lambda} \right) , \tag{7}$$

respectively its associated integral equation

$$C_{\mathcal{T}}(x,t) = F(x) \int_0^t C_{\mathcal{A}}(\tau)\, e^{-\frac{F(x)}{\lambda}(t-\tau)}\, d\tau , \tag{8}$$

where F denotes the MBF, $C_{\mathcal{A}}$ represents the left ventricular blood over time and λ is a fixed partition coefficient (e.g. $\lambda = 0.96$).

Interesting properties of $\mathbf{C}_{\mathcal{T}}$

Interesting properties of $\mathbf{C}_{\mathcal{T}}$

- Equation (8) represents a nonlinear operator $\mathbf{C}_{\mathcal{T}}(F, \mathrm{C}_{\mathcal{A}})$ with solution $\mathrm{C}_{\mathcal{T}}$

Interesting properties of $\mathbf{C}_{\mathcal{T}}$

- Equation (8) represents a nonlinear operator $\mathbf{C}_{\mathcal{T}}(F, \mathrm{C}_{\mathcal{A}})$ with solution $\mathrm{C}_{\mathcal{T}}$
- The operator $\mathbf{C}_{\mathcal{T}}$ represented by (8) offers the following interesting properties

Properties of $\mathbf{C}_{\mathcal{T}}$

- $\mathbf{C}_{\mathcal{T}} : \mathcal{D}_p(\mathbf{C}_{\mathcal{T}}) \to L_p(\Omega \times [0, T])$ is non-negative,

Interesting properties of $\mathbf{C}_{\mathcal{T}}$

- Equation (8) represents a nonlinear operator $\mathbf{C}_{\mathcal{T}}(F, \mathrm{C}_{\mathcal{A}})$ with solution $\mathrm{C}_{\mathcal{T}}$
- The operator $\mathbf{C}_{\mathcal{T}}$ represented by (8) offers the following interesting properties

Properties of $\mathbf{C}_{\mathcal{T}}$

- $\mathbf{C}_{\mathcal{T}} : \mathcal{D}_p(\mathbf{C}_{\mathcal{T}}) \to L_p(\Omega \times [0, T])$ is non-negative,
- $\mathbf{C}_{\mathcal{T}} : \mathcal{D}_p(\mathbf{C}_{\mathcal{T}}) \to L_p(\Omega \times [0, T])$ is well-defined and L_p-continuous on $\mathcal{D}_p(\mathbf{C}_{\mathcal{T}})$,

Interesting properties of $\mathbf{C}_{\mathcal{T}}$

- Equation (8) represents a nonlinear operator $\mathbf{C}_{\mathcal{T}}(F, \mathrm{C}_{\mathcal{A}})$ with solution $\mathrm{C}_{\mathcal{T}}$
- The operator $\mathbf{C}_{\mathcal{T}}$ represented by (8) offers the following interesting properties

Properties of $\mathbf{C}_{\mathcal{T}}$

- $\mathbf{C}_{\mathcal{T}} : \mathcal{D}_p(\mathbf{C}_{\mathcal{T}}) \to L_p(\Omega \times [0, T])$ is non-negative,
- $\mathbf{C}_{\mathcal{T}} : \mathcal{D}_p(\mathbf{C}_{\mathcal{T}}) \to L_p(\Omega \times [0, T])$ is well-defined and L_p-continuous on $\mathcal{D}_p(\mathbf{C}_{\mathcal{T}})$,
- $\mathbf{C}_{\mathcal{T}} : \mathcal{D}_p(\mathbf{C}_{\mathcal{T}}) \cap (L_{2p}(\Omega) \times L_{2p}([0, T])) \to L_p(\Omega \times [0, T])$ is Fréchet differentiable, with

$$\mathcal{D}_p(\mathbf{C}_{\mathcal{T}}) := \{F \in L_p(\Omega), \mathrm{C}_{\mathcal{A}} \in L_p([0, T]) \mid F \geq 0, \mathrm{C}_{\mathcal{A}} \geq 0\} \qquad (9)$$

and for $p \geq 1$

Quantification as a Nonlinear Inverse Problem

Quantification as a Nonlinear Inverse Problem

- Recall the basic principle of novel MBF quantification

$$p(x,t) \xrightarrow[\text{nonlinear}]{G} u(x,t) \xrightarrow[\text{linear}]{B} f(\sigma,\theta,t)$$

Inversion of

nonlinear operator G

Quantification as a Nonlinear Inverse Problem

- Recall the basic principle of novel MBF quantification

$$p(x,t) \xrightarrow[\text{nonlinear}]{G} u(x,t) \xrightarrow[\text{linear}]{B} f(\sigma,\theta,t)$$

Inversion of

nonlinear operator G

- Based on (8) we introduce a new operator G that produces an image sequence u from physiological parameters p, i.e. $G(p) = u$, e.g.

Exemplary Operator G

$$G(F, C_{\mathcal{A}}, C_{\mathcal{V}}) = \mathbf{C}_{\mathcal{T}}\,|_{\mathcal{T}} + C_{\mathcal{A}}\,|_{\mathcal{A}} + C_{\mathcal{V}}\,|_{\mathcal{V}} \qquad (10)$$

- Since we are interested in the parameters p we now need to consider the inverse problem

Modified Minimization Problem

$$p \in \arg\min_{p \in \mathcal{P}} \left\{ KL_T(f, BG(p)) + \mathcal{R}(p) \right\} , \tag{11}$$

$$KL_T(f, Bu) = \int_0^T \int_\Sigma f \log\left(\frac{f}{Bu}\right) + Bu - f \, dx \, dt , \tag{12}$$

with $\mathcal{P}$ denoting the domain of parameters and $\mathcal{R}$ guaranteeing regularization to the parameters p.

- This minimization problem can be rewritten to the constrained problem

Constrained problem

$$
\begin{aligned}
KL_T(f, Bu) + \mathcal{R}(p) \rightarrow \min_{p \in \mathcal{P}} \\
\text{subject to } u = G(p)|_{\mathcal{H}} \,,
\end{aligned}
\tag{13}
$$

- This minimization problem can be rewritten to the constrained problem

Constrained problem

$$KL_T(f, Bu) + \mathcal{R}(p) \to \min_{p \in \mathcal{P}} \quad \text{subject to } u = G(p)|_{\mathcal{H}}\,, \tag{13}$$

- Rewritten in terms of a Lagrange multiplier with L_2 dual product we obtain

Lagrange multiplier

$$\mathcal{L}(u, p; q) = KL_T(f, Bu) + \mathcal{R}(p) + \langle G(p) - u, q \rangle_{L_2([0,T]\times\mathcal{H})} \tag{14}$$

- The optimality conditions of (14) are

Optimality conditions

$$q = B^*1 - B^*\left(\frac{f}{Bu}\right), \tag{15}$$

$$(G')^*(p)\, q = -\mathcal{R}'(p), \tag{16}$$

$$u = G(p). \tag{17}$$

- The optimality conditions of (14) are

Optimality conditions

$$q = B^*1 - B^*\left(\frac{f}{Bu}\right), \tag{15}$$

$$(G')^*(p)\, q = -\mathcal{R}'(p), \tag{16}$$

$$u = G(p). \tag{17}$$

- If we multiply (15) with u this yields

Analytical equation for Lagrange multiplier

$$0 = uB^*1 - uB^*\left(\frac{f}{Bu}\right) - uq. \tag{18}$$

Reminder

Reminder

$$
\begin{aligned}
0 &= uB^*1 - uB^*\left(\frac{f}{Bu}\right) - uq \\
&= B^*1\left(u \underbrace{- \frac{u}{B^*1}\left(\frac{f}{Bu}\right)}_{*}\right) - uq
\end{aligned}
$$

Reminder

$$
\begin{aligned}
0 &= uB^*1 - uB^*\left(\frac{f}{Bu}\right) - uq \\
&= B^*1\left(u \underbrace{-\frac{u}{B^*1}\left(\frac{f}{Bu}\right)}_{*}\right) - uq
\end{aligned}
$$

- Adding u to * and setting this equation to zero satisfies the optimality condtion of the Kullback-Leibler functional (5) for each timestep t

Reminder

$$
\begin{aligned}
0 &= uB^*1 - uB^*\left(\frac{f}{Bu}\right) - uq \\
&= B^*1\left(u \underbrace{- \frac{u}{B^*1}\left(\frac{f}{Bu}\right)}_{*}\right) - uq
\end{aligned}
$$

- Adding u to * and setting this equation to zero satisfies the optimality condtion of the Kullback-Leibler functional (5) for each timestep t
- Idea:

Reminder

$$
\begin{aligned}
0 &= uB^*1 - uB^*\left(\frac{f}{Bu}\right) - uq \\
&= B^*1\left(u \underbrace{- \frac{u}{B^*1}\left(\frac{f}{Bu}\right)}_{*}\right) - uq
\end{aligned}
$$

- Adding u to * and setting this equation to zero satisfies the optimality condtion of the Kullback-Leibler functional (5) for each timestep t
- Idea: Replace * with the discrete solution of (5) and solve equation (18) with the iterative scheme

Semidiscrete equation for Lagrange multiplier

$$u_k q = B^* 1 \left(u_{k+1} - u_{k+\frac{1}{2}} \right) \tag{19}$$

$$\Leftrightarrow u_{k+1} = u_{k+\frac{1}{2}} + \frac{u_k q}{B^* 1}\,, \tag{20}$$

to u_{k+1}, with $u_{k+\frac{1}{2}}$ being the EM update (6) of u_k.

Semidiscrete equation for Lagrange multiplier

$$u_k q = B^*1 \left(u_{k+1} - u_{k+\frac{1}{2}} \right) \tag{19}$$

$$\Leftrightarrow u_{k+1} = u_{k+\frac{1}{2}} + \frac{u_k q}{B^*1}\,, \tag{20}$$

to u_{k+1}, with $u_{k+\frac{1}{2}}$ being the EM update (6) of u_k.

- We set $\kappa(x,t) := \frac{B^*1}{u_k}$

- Solving (20) to u_{k+1} can be seen as solving the minimization problem

Semidiscrete Minimization Problem 1

$$u_{k+1} \in \underset{u \in L_2([0,T]\times\Omega)}{\arg\min} \left\{ \frac{1}{2} \int_0^T \int_\Omega \left(u - u_{k+\frac{1}{2}} \right)^2 \kappa \, dxdt - \langle u, q \rangle_{L_2([0,T]\times\Omega)} \right\}. \tag{21}$$

- Applying (17) results in

Semidiscrete Minimization Problem 2

$$p \in \underset{p \in \mathcal{P}}{\arg\min} \left\{ \frac{1}{2} \int_0^T \int_{\mathcal{H}} \left(G(p) - u_{k+\frac{1}{2}} \right)^2 \kappa \, dxdt \right. \\ \left. - \langle G(p), q \rangle_{L_2([0,T]\times\mathcal{H})} \right\}, \tag{22}$$

subject to $u_{k+1} = G(p)|_{\mathcal{H}}$.

- It is easy to see that the Fréchet derivative of $\langle G(p), q \rangle$ in p simply equals $G^{'}(p)^{*}q$

- It is easy to see that the Fréchet derivative of $\langle G(p), q\rangle$ in p simply equals $G'(p)^* q$
- Together with (16) we obtain the reduced problem

Semidiscrete Minimization Problem 3

$$p \in \operatorname*{arg\,min}_{p\in\mathcal{P}} \left\{ \frac{1}{2} \int_0^T \int_{\mathcal{H}} \left(G(p) - u_{k+\frac{1}{2}} \right)^2 \kappa \, dxdt + \mathcal{R}(p) \right\} . \qquad (23)$$

- A solution of (23) can be obtained by computing the optimality conditions of the Lagrange multiplier

Parameter Identification Problem

$$\mathcal{L}_k(u,p;\mu) = \frac{1}{2}\int_0^T\int_\Omega \kappa\left(u-u_{k+\frac{1}{2}}\right)^2 dxdt + \mathcal{R}(p) + \int_0^T\int_\mathcal{H} (G(p)-u)\,\mu dxdt \tag{24}$$

- A solution of (23) can be obtained by computing the optimality conditions of the Lagrange multiplier

Parameter Identification Problem

$$\mathcal{L}_k(u,p;\mu) = \frac{1}{2}\int_0^T \int_\Omega \kappa \left(u - u_{k+\frac{1}{2}}\right)^2 dxdt + \mathcal{R}(p) + \int_0^T \int_\mathcal{H} \left(G(p) - u\right) \mu dxdt \tag{24}$$

- The optimality conditions $\partial_u \mathcal{L}_k(u,p;\mu) = 0$ and $\partial_\mu \mathcal{L}_k(u,p;\mu) = 0$ can be computed analytically

- The optimality conditions for p can be computed iteratively, e.g. via a Landweber iteration of the gradient descent of $\partial_p \mathcal{L}_k$

Computational Parameter Identification

Given a set of n parameters $p = \left(p^i\right)_{i=\{1,\ldots,n\}}$, each parameter can be computed via

$$p^i_{j+1} = p^i_j - \tau\, \partial_{p^i} \mathcal{L}_k(u, p_j; \mu)\,, \tag{25}$$

with $\tau > 0$ being small, such that $\partial_u \mathcal{L}_k(u, p_j; \mu) = 0$ and $\partial_\mu \mathcal{L}_k(u, p_j; \mu) = 0$.

- The optimality conditions for p can be computed iteratively, e.g. via a Landweber iteration of the gradient descent of $\partial_p \mathcal{L}_k$

Computational Parameter Identification

Given a set of n parameters $p = \left(p^i\right)_{i=\{1,\ldots,n\}}$, each parameter can be computed via

$$p^i_{j+1} = p^i_j - \tau \, \partial_{p^i} \mathcal{L}_k(u, p_j; \mu) \,, \tag{25}$$

with $\tau > 0$ being small, such that $\partial_u \mathcal{L}_k(u, p_j; \mu) = 0$ and $\partial_\mu \mathcal{L}_k(u, p_j; \mu) = 0$.

- Iteration is stopped after m iterations (e.g. if $\|p_m - p_{m-1}\| < \varepsilon$, ε small)

- The optimality conditions for p can be computed iteratively, e.g. via a Landweber iteration of the gradient descent of $\partial_p \mathcal{L}_k$

Computational Parameter Identification

Given a set of n parameters $p = \left(p^i\right)_{i=\{1,\dots,n\}}$, each parameter can be computed via

$$p^i_{j+1} = p^i_j - \tau\, \partial_{p^i} \mathcal{L}_k(u, p_j; \mu)\,, \tag{25}$$

with $\tau > 0$ being small, such that $\partial_u \mathcal{L}_k(u, p_j; \mu) = 0$ and $\partial_\mu \mathcal{L}_k(u, p_j; \mu) = 0$.

- Iteration is stopped after m iterations (e.g. if $\|p_m - p_{m-1}\| < \varepsilon$, ε small) $\Rightarrow$ $u_{k+1} = G(p_m)$

- The optimality conditions for p can be computed iteratively, e.g. via a Landweber iteration of the gradient descent of $\partial_p \mathcal{L}_k$

Computational Parameter Identification

Given a set of n parameters $p = \left(p^i\right)_{i=\{1,\ldots,n\}}$, each parameter can be computed via

$$p^i_{j+1} = p^i_j - \tau \, \partial_{p^i} \mathcal{L}_k(u, p_j; \mu) \,, \tag{25}$$

with $\tau > 0$ being small, such that $\partial_u \mathcal{L}_k(u, p_j; \mu) = 0$ and $\partial_\mu \mathcal{L}_k(u, p_j; \mu) = 0$.

- Iteration is stopped after m iterations (e.g. if $\|p_m - p_{m-1}\| < \varepsilon$, ε small) $\Rightarrow u_{k+1} = G(p_m)$

$$\boxed{\text{EM}} \rightarrow \boxed{u_{k+\frac{1}{2}}} \rightarrow \boxed{\text{PI}} \rightarrow \boxed{p_m} \rightarrow \boxed{u_{k+1}}$$

Ill-posedness and Regularization

Ill-posedness and Regularization

- As most inverse problems, the inverse problem of MBF quantification is ill-posed

Ill-posedness and Regularization

- As most inverse problems, the inverse problem of MBF quantification is ill-posed
- Hence, appropriate regularization is needed:

Tikhonov Regularization

$$\mathcal{R}_T(p^i) = \frac{\alpha}{2} \int_{\Psi_i} \left(p^i(s) - p^i_*(s)\right)^2 ds \tag{26}$$

with $\alpha > 0$

Ill-posedness and Regularization

- As most inverse problems, the inverse problem of MBF quantification is ill-posed
- Hence, appropriate regularization is needed:

Tikhonov Regularization

$$\mathcal{R}_T(p^i) = \frac{\alpha}{2} \int_{\Psi_i} \left(p^i(s) - p^i_*(s)\right)^2 ds \qquad (26)$$

with $\alpha > 0$

- With given a-priori knowledge p^i_*, Tikhonov regularization secures that computed parameters p^i are bounded (e.g. p^i_* can be a typical average value for the parameter p^i)

- Disadvantage of Tikhonov regularization: reconstructed parameters are bounded but can still contain oscillating patterns

- Disadvantage of Tikhonov regularization: reconstructed parameters are bounded but can still contain oscillating patterns
- To obtain smooth, non-oscillating parameter reconstructions, the H^1-norm can be applied as a regularizer:

H^1-Regularization

$$\mathcal{R}_{H_1}(p^i) = \left\| p^i - p^i_* \right\|^2_{H_1} = \mathcal{R}_T(p^i) + \frac{\alpha}{2} \sum_{j=1}^{n} \int_{\Psi_i} \left(\frac{\partial}{\partial s_j} p^i(s) \right)^2 ds \tag{27}$$

with $\alpha > 0$

- Disadvantage of Tikhonov regularization: reconstructed parameters are bounded but can still contain oscillating patterns
- To obtain smooth, non-oscillating parameter reconstructions, the H^1-norm can be applied as a regularizer:

H^1-Regularization

$$\mathcal{R}_{H_1}(p^i) = \left\|p^i - p_*^i\right\|_{H_1}^2 = \mathcal{R}_T(p^i) + \frac{\alpha}{2}\sum_{j=1}^{n}\int_{\Psi_i}\left(\frac{\partial}{\partial s_j}p^i(s)\right)^2 ds \tag{27}$$

with $\alpha > 0$

- Discontinuities are not preserved; this might not be a disadvantage for this type of application, due to cardiac motion

- With added H^1-Regularization we are able to prove existence of a solution and continuous dependency on the input data

- With added H^1-Regularization we are able to prove existence of a solution and continuous dependency on the input data
- Uniqueness would be desireable, to obtain a completely well-posed problem

- With added H^1-Regularization we are able to prove existence of a solution and continuous dependency on the input data
- Uniqueness would be desireable, to obtain a completely well-posed problem
- Unfortunately, $\mathbf{C}_{\mathcal{T}}$ is not a (strictly) convex operator

- With added H^1-Regularization we are able to prove existence of a solution and continuous dependency on the input data
- Uniqueness would be desireable, to obtain a completely well-posed problem
- Unfortunately, $\mathbf{C}_{\mathcal{T}}$ is not a (strictly) convex operator
  $\Rightarrow$ No guarantee of global minima

Synthetic Data

Synthetic Data

- We generated a very simple synthetic dataset with the following simple segmentation

Segmentation

(a) $\mathcal{A}$ (b) $\mathcal{V}$ (c) $\mathcal{T}$

Figure: Simple Segmentation

- We generated a synthetic dataset with the following parameters

- We generated a synthetic dataset with the following parameters

Parameters

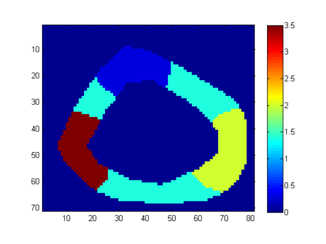

(a) MBF F in ml/min/mg

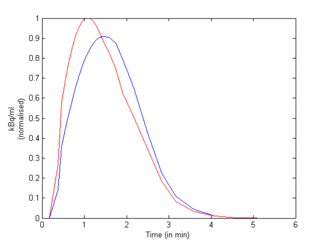

(b) $C_{\mathcal{A}}$ and $C_{\mathcal{V}}$ in kBq/ml over time

Figure: Exact parameters

- We generated a synthetic dataset with the following parameters

Parameters

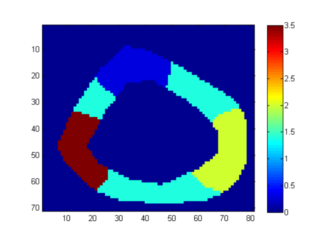

(a) MBF F in ml/min/mg

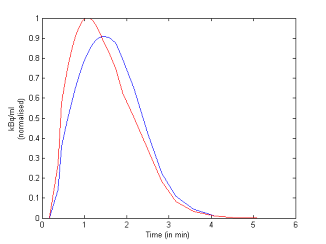

(b) $C_{\mathcal{A}}$ and $C_{\mathcal{V}}$ in kBq/ml over time

Figure: Exact parameters

- Partition coefficient $\lambda = 0.96$ has been set to a fixed value

- We set $u(x,t) = G(F, \mathsf{C}_{\mathcal{A}}, \mathsf{C}_{\mathcal{V}})|_{\mathcal{H}} + 0|_{\Omega\setminus\mathcal{H}}$

- We set $u(x,t) = G(F, \mathrm{C}_{\mathcal{A}}, \mathrm{C}_{\mathcal{V}})|_{\mathcal{H}} + 0|_{\Omega\setminus\mathcal{H}}$
- We generate $\wp(Bu) = f$ via a simple Monte-Carlo algorithm with a maximum number of counts of 61415

- We set $u(x,t) = G(F, C_{\mathcal{A}}, C_{\mathcal{V}})|_{\mathcal{H}} + 0|_{\Omega\setminus\mathcal{H}}$
- We generate $\wp(Bu) = f$ via a simple Monte-Carlo algorithm with a maximum number of counts of 61415
- The following image shows the 9-th frame of a standard EM-reconstruction (without any regularization) of the synthetic PET data

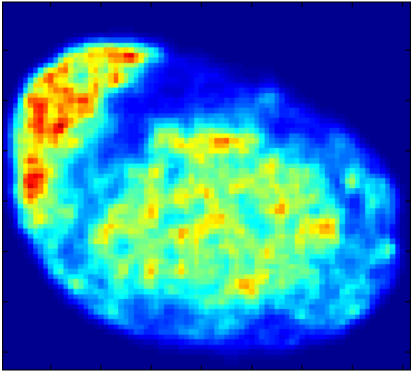

Reconstructions

Reconstructions

Comparison: Exact vs Reconstruction

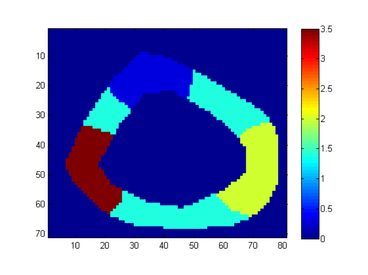

(a) Exact MBF

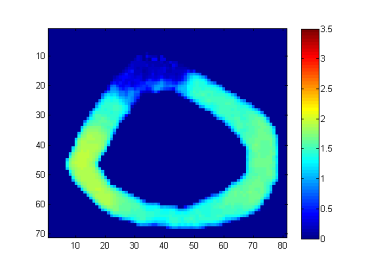

(b) Reconstructed MBF

Figure: Reconstructions

Reconstructions

Comparison: Complete Image Sequences

Synthetic Data

- Video animated with the help of Jahn ☺

Real $H_2{}^{15}O$ PET Data

Real $H_2{}^{15}O$ PET Data

- To conclude this talk we want to present some computational results for real $H_2{}^{15}O$ PET data

Real $H_2{}^{15}O$ PET Data

- To conclude this talk we want to present some computational results for real $H_2{}^{15}O$ PET data
- The data is obtained from a two-dimensional transaxial slice containing the cardiovascular region

Real $H_2{}^{15}O$ PET Data

- To conclude this talk we want to present some computational results for real $H_2{}^{15}O$ PET data
- The data is obtained from a two-dimensional transaxial slice containing the cardiovascular region
- The (rough) segmentation has been done manually with the help of EM-TV reconstructions

Segmentation

Segmentation

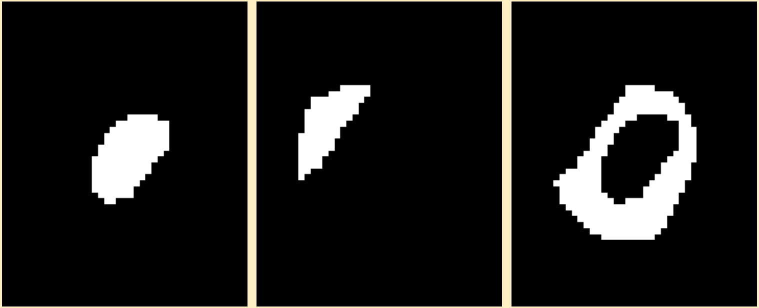

(a) $\mathcal{A}$ (b) $\mathcal{V}$ (c) $\mathcal{T}$

Figure: Simple Segmentation obtained from EM-TV Reconstructions

Reconstructions

Reconstructions - Rest

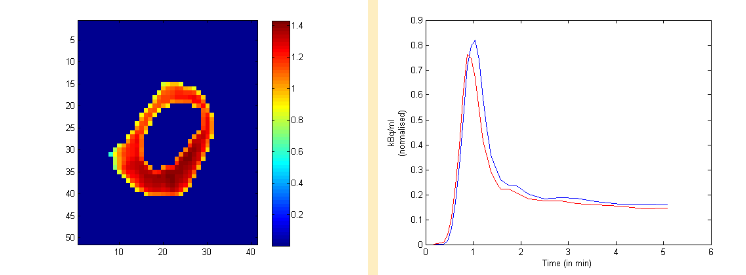

(a) MBF F

(b) Arterial Input $C_{\mathcal{A}}$ & Venous Input $C_{\mathcal{V}}$

Figure: Reconstructions obtained from real $H_2{}^{15}O$ PET data

Reconstructions

Reconstruction of Complete Image Sequence

Real Data

- Again, the video was animated with the help of Jahn ☺

Thank you for your attention!